Vol. 21, No. 1(2022) Proc2607
Revista Mexicana de Ingeniería Química

Development and characterization of an alternative control system to study separately oxygen and momentum transfer effects in stirred tank bioreactors

Desarrollo y caracterización de un sistema alternativo de control para estudiar por separado los efectos de transferencia de oxígeno y de cantidad de movimiento en biorreactores de tanque agitado

J.D. López-Taborda[1], A. Vargas-Zapata[2], J.F. Ramírez-Vargas[2], N.A. Valdez-Cruz[3], M.A. Trujillo-Roldán[3], F. Orozco-Sánchez[1]*

[1]*Facultad de Ciencias, Universidad Nacional de Colombia - Sede Medellín, Cra. 65 # 59ª-110, Medellín, Colombia.*
[2]*Industrias Centricol S.A.S., Calle 19A # 81B-51, Barrio Belén, Medellín, Colombia.*
[3]*Programa de Investigación de Producción de Biomoléculas, Universidad Nacional Autónoma de México, Av. Universidad 3000, Cd. Universitaria, Coyoacán, 04510, Ciudad de México, México.*

Received: September 22, 2021; Accepted: February 4, 2022

Abstract

Control systems for dissolved oxygen tension (DOT) in stirred tank bioreactors (STB) commonly manipulate gas flow or agitation speed. However, this strategy alters hydrodynamic conditions thus interrelating oxygen and momentum transfer effects in the culture. The aim of this study was to develop an alternative DOT control system and characterize its performance in terms of control error and energy dissipation rates. Hence, a novel control algorithm was designed with three mass flow controllers by manipulating oxygen partial pressure at constant gas flow and agitation. The developed system was evaluated with an *Escherichia coli* culture and was found to control DOT with an absolute error below 2%. When compared to a standard controller, 42% lower accumulated error was found. The energy dissipation rate (EDR) by agitation was 0.06 W kg^{-1}, and EDR variations via bubble wake and bursting were diminished with respect to the standard. Additionally, the system effectively responded to perturbations on set point (30, 50, 80%) and agitation (200, 500, 1000 rpm). To the best of authors' knowledge, this is the first characterization of a DOT controller in terms of EDR and control error that could be used to study oxygen and momentum transfer effects separately in STB.

Keywords: Dissolved oxygen, mass flow controller, constant rpm, control algorithm, oxygen controllability, energy dissipation rate.

Resumen

Los sistemas de control para la tensión de oxígeno disuelto (DOT) en biorreactores de tanque agitado (STB) generalmente manipulan el flujo de gas o la velocidad de agitación. Sin embargo, esta estrategia perturba las condiciones hidrodinámicas, interrelacionando los efectos de la transferencia de oxígeno y momento en el cultivo. El objetivo de este trabajo fue desarrollar un sistema de control de oxígeno alternativo y caracterizar su comportamiento en términos de error de control y velocidades de disipación de energía (EDR). Para esto, se diseñó un nuevo algoritmo de control utilizando tres controladores de flujo másico y manipulando la presión parcial del oxígeno bajo flujo de gas y agitación constantes. El sistema desarrollado controló precisamente la DOT con un error menor al 2% en un cultivo de *Escherichia coli*. El error acumulado de control fue 42% menor que aquel de un controlador estándar comercial. La velocidad de disipación de energía (EDR) por agitación se mantuvo a 0.06 W/kg, y se disminuyeron las variaciones de EDR por el ascenso y el estallamiento de las burbujas respecto al estándar. Adicionalmente, el sistema respondió efectivamente a perturbaciones en el *set-point* (30, 50 y 80%) y la agitación (200, 500 y 1000 rpm). Según el conocimiento de los autores, esta es la primera caracterización de un controlador de DOT en términos de velocidad de disipación de energía y error de control que puede ser utilizada para estudiar la transferencia de oxígeno y cantidad de movimiento en STB.

Palabras clave: Tensión de oxígeno disuelto, controlador de flujo másico, rpm constantes, algoritmo de control, controlabilidad de oxígeno, velocidad de disipación de energía.

* *Corresponding author. E-mail*: feorozco@unal.edu.co
https://doi.org/10.24275/rmiq/Proc2607
ISSN:1665-2738, *issn-e*: 2395-8472

1 Introduction

Dissolved oxygen tension (DOT) is an imperative parameter that affects biomass and product productivities in biological processes occurring in stirred tank bioreactors (STBs) (Félix Garcia-Ochoa & Gomez, 2009; Martínez-Hernández *et al*., 2020). The supply of oxygen to the liquid broth has been a main challenge in bioreactor operation (Alford, 2006) because mass, heat, and momentum transfer phenomena are dynamically correlated (Ferreira *et al*., 2017). The dynamics of oxygen in STB is mathematically represented with an oxygen mass balance (Eq. 1). Here, the change in oxygen concentration in time (dC_{O2}/dt) corresponds to the difference between oxygen transfer rate (OTR) from the inlet gas to the broth, and the oxygen uptake rate (OUR) from cells (Orozco-Sánchez *et al*., 2011). The OTR involves the volumetric mass transfer coefficient (k_La) and a driving force corresponding to the difference in oxygen concentration in the bubble interface (C^*_{O2}) and the inner liquid (C_{O2}). Conversely, the OUR depends on biomass concentration (X) and oxygen consumption rate (qo) (Akesson & Hagander, 1998; Gomes & Menawat, 2000; Schlüter & Deckwer, 1992). Simultaneously, k_La is significantly dependent on operation variables such as power input, aeration rate, gas sparging, pH, and temperature (Maia *et al*., 1999; Martinov *et al*., 2008; Schaepe *et al*., 2013). Indeed, changes on cell growth rate, bioreactor pressure, and addition of acid, base, or antifoam constitute perturbations for DOT control in the culture.

$$\frac{dC_{O2}}{dt} = OTR - OUR = k_La(C^*_{O2} - C_{O2}) - q_oX \quad (1)$$

Plant, mammalian, and fungal cells are generally reported to be sensitive to hydrodynamics and shear conditions in STB, which are derived from variations in operational parameters (García-Ochoa *et al*., 2015; Hua *et al*., 1993). For example, alteration of mixing and gas flow generates different events such as shear forces derived from agitation, or formation, rising and bursting of gas bubbles (Dunlop & Namdev, 1994; Neunstoecklin *et al*., 2015; Wu, 1995). These events are related with hydrodynamic conditions that can be characterized in terms of energy dissipation, shear stress, and turbulent Eddy length. Specifically, the energy dissipation rate (EDR) is used as a common parameter to quantify the rate of work performed on a liquid volume by the surroundings and can be related to cell damage and hydrodynamic stress in bioreactors (Chalmers, 2015; Walls *et al*., 2017). The stressing levels derived from hydrodynamic conditions are reported to exhibit lethal and sub-lethal effects in cells and cause death, apoptosis, or stimulation of secondary metabolic routes (Trujillo-Roldán & Valdez-Cruz, 2006). Hence, although hydrodynamic stress is reported to decrease cell viability for plant and animal cells, it is also used as a strategy to increase secondary metabolite production (Busto *et al*., 2008; Villegas-Velásquez *et al*., 2017).

During a bioreactor cultivation, persistent variations on OTR must be performed to equilibrate OUR, thereby maintaining adequate DOT levels for cell growth and metabolite production (García-Cabrera *et al*., 2021). For example, common strategies to control DOT in STB use agitation speed or gas flow as manipulated variables (Akesson & Hagander, 1998; Raffo-Durán *et al*., 2014). However, these strategies directly affect momentum transfer conditions since they perturbate k_La and hydrodynamics. Thus, the DOT control system generates an integrated response on cells that is derived from oxygen and momentum transfer conditions (Félix Garcia-Ochoa & Gomez, 2009).

Alternative DOT control strategies have been developed at constant gas flow and agitation speed (De León-Rodríguez *et al*., 2010; Smith *et al*., 1990; Trujillo Roldán *et al*., 2001), and control systems are commercially available. However, they have not been characterized in terms of EDR and control error. Therefore, it is still not clear how to examine separately oxygen and momentum transfer effects by using the control strategy in STB. Hence, the aim of the study was to develop an alternative DOT control system and characterize its performance in terms of EDR and control error; thus, allowing further study of oxygen and momentum transfer effects separately in STBs.

2 Materials and methods

2.1 *Equipment and control algorithm for the alternative system*

A mixture of air, pure oxygen, and pure nitrogen was used to feed the bioreactor. Each gas was filtered from the source via a 0.2-μm filter (PTFE PN 4250, Pall Corporation, New York, USA), and each flow was controlled by a mass flow controller (MFC) (Sierra Instruments Inc. SmartTrak series 50, Monterey, CA,

USA). Gases were dynamically mixed up with a three-way valve. The DOT was measured by a polarographic Oxyferm FDA-ARC-325 electrode (Hamilton, Reno, NV, USA). A programmable logic controller (PLC, Vision 130, Unitronics, Israel) was used to program the proportional-integral-derivative (PID) loops and the control algorithm. All the system components were assembled by Industrias Centricol Ltda. (Medellín, Colombia).

An open loop for the control system was done at operation conditions. Then, a novel algorithm based on the DOT reaction curve was developed. The control objective was to maintain the DOT at a desired percentage at constant gas flow and agitation speed. For this, a cascade control strategy proposed in extant studies was used (De León-Rodríguez *et al*., 2010; Trujillo Roldán *et al*., 2001).

2.2 Evaluation of oxygen controllability

2.2.1 Model culture, bioreactor configuration and analytics

Escherichia coli BL21 culture was used as a model to examine DOT control. The bacteria is not reported to suffer major physiological effects due fluid mechanical stresses in STB (Chamsartra *et al*., 2005; Hewitt *et al*., 1998). However, it was selected as a model because their cultures exhibit a high demand for oxygen (typical up to 23 mol_{O2} kg^{-1} h^{-1}) and allow fast and sensitive response to oxygen dynamics, and thus it constitutes an exigent system with respect to DOT controllability (Felix Garcia-Ochoa *et al*., 2010). All cultures were grown in Luria Bertani (LB) medium containing tryptone (10 g L^{-1}), yeast extract (5 g L^{-1}), and sodium chloride (10 g L^{-1}). Prior to sterilization, media were always set to a pH of 7.4 via the addition of NaOH (2 N). A 3-L stirred tank bioreactor vessel (Applikon Biotechnology BV, Delft, The Netherlands), with 2-L working volume was used. The vessel was equipped with a Rushton impeller at the end of the shaft (Di/T = 0.4) and a gas sparger with seven holes. Operation parameters other than DOT were controlled with an ADI1010 biocontroller (Applikon Biotechnology BV). Temperature was controlled at 37°C by blanket heating. The pH was controlled at 7.2 by automatic addition of NaOH (2 N) and H_2SO_4 (1 N). Finally, foam was manually disrupted when necessary, via the addition of food grade antifoam (10% v/v). For each inoculum, 100 μL of cryopreserved bacteria at -80°C were added to a 250-mL shake flask containing 50 mL of LB medium. The shake flask was closed with a 7.0-g cotton plug. The inoculum was grown for 12 h at 37°C with agitation at 200 rpm by using an orbital shaker (Centricol LTDA, Medellín, Colombia). All biomass growth kinetics were obtained via measuring optical density (OD_{600}) at 600 nm (Genesys 20 ThermoScientific, Waltham, MA, USA). Dilutions were performed when required, and thus the OD_{600} measurement was always lower than 0.8. Data from ADI1010 controller were obtained by BioXpert Lite© 2008 software (Applikon Biotechnology BV, Delft, The Netherlands). Finally, DOT data were obtained using an Unitronics DataXport software (Industrias Centricol Ltda. Company, Medellín, Colombia).

2.2.2 Comparison with a standard DOT control strategy

Using a standard DOT control strategy, cultivations were done to compare the performance of the developed algorithm. Standard control of DOT was performed by manipulating gas flow with a solenoid valve (ADI 1010, Applikon Biotechnology BV, Delft, The Netherlands). Agitation speed and maximum gassing were set to reach an initial k_La of 70 h^{-1}.

2.2.3 Performance of the system and DOT controllability

The performance of the standard and the alternative control strategies were compared in terms of control efficiency in the cultures. Thus, control absolute errors (e) were calculated at every minute. Errors were defined as the difference between the set point (SP) and dynamic DOT as shown by Eq. (2). Additionally, total accumulated errors of the runs were calculated using Eq. (3). The errors were plotted and compared.

$$e(t) = |SP_{DOT} - DOT(t)| \tag{2}$$

$$\text{Total accumulated error} = \sum_{0}^{t} e_i(t) \tag{3}$$

The experimental response of the alternative DOT control system was proven by applying different perturbations on the SP and agitation rate. Three different agitation speeds were used (200, 500, and 1000 rpm) at different culture stages. The initial k_La was also measured using the dynamic method. The stabilization of the DOT prior to each perturbation was plotted. Biomass growth was compared with that in previous treatments to determine whether the control system affected the growth of cells.

2.3 Calculation of energy dissipation rates

2.3.1 Energy dissipation rate by agitation

The control strategies were characterized in terms of energy dissipation rates (EDR). Thus, the power delivered from the impellers to the liquid broth (P) was estimated via calculating the power number (P_o) with an empiric correlation (Eq. 4). The equation was previously derived for a single Rushton impeller and a geometric relation of B/T=0.25 (which was accomplished for the study configuration) (Bujalski, 1986; Nienow, 1998; Villegas-Velásquez *et al*., 2017).

$$P_o = 2.5\left(\frac{x}{D}\right)^{-0.2}\left(\frac{T}{T_o}\right)^{0.065} \tag{4}$$

Subsequently, the definition of the power number (P_o) was used to calculate the ungassed power input (P) in Eq. (5) (Doran, 1995) as follows:

$$P = P_o \rho N^3 D^5 \tag{5}$$

When the broth is gasified, the power input to the culture decreases because the presence of gas bubbles reduces broth density and viscosity and causes hydrodynamic changes around the impeller (Doran, 1995). This phenomena cannot be mathematically predicted although empirical correlations have been proposed relating aerated and unaerated power input (Gill *et al*., 2008). The correlation proposed by Smith (2006) from data obtained by Warmoeskerken and Smith (1982) was used to calculate the gassed power input (P_g) from the previously calculated ungassed power input (P). The correlation uses the Froude number (F_r) and flow number (F_{lg}) as shown in Eq. 6-8 (Devi & Kumar, 2017) and can be applied for a single Rushton turbine operating in homogeneous (small bubbles) and heterogeneous (bubbles > 3 cm) gas dispersions in stirred vessels. The equation is obtained for superficial velocities of gas between 0.0 and 0.1 m s^{-1} (Gezork *et al*., 2000; Smith, 2006) as follows:

$$\frac{P_g}{P} = 0.18 Fr^{-0.2} F_{lg}^{-0.25} \tag{6}$$

$$Fr = N^2 D/g \tag{7}$$

$$F_{lg} = F_g/ND^3 \tag{8}$$

Using the corresponding calculated gassed or ungassed power input (P_c), the average EDR due to agitation for the two control systems were calculated for each time sample based on Eq. (9) as follows:

$$\varepsilon_{agit|avg} = P_c/\rho V_L \tag{9}$$

2.3.2 Energy dissipation rate by gassing

To compare the control strategies in terms of gasification effects, two phenomena were considered. First, the EDR that a wake behind a bubble inputs to the liquid when rising from sparger to surface was calculated as the EDR by bubble wake (Chisti, 2000). Second, an analysis based on the energy inputted by a bubble bursting at the surface of the liquid was performed (Boulton-Stone & Blake, 1993; Chisti, 2000; Garcia-Briones *et al*., 1994; Walls *et al*., 2017). The analysis of EDR by gassing depends on bubble size, and thus average bubble diameters were measured for different agitation/aeration conditions in both systems. Thus, videos were obtained at a fixed shot with a professional camera (Sony XDCAM) using a resolution corresponding to 1080/60i at 50 fps, an ISO of 15 dB, and shutter speed of 1500. The images were used to measure the bubble diameters at different gas flows with the Image J® image analyzer. The average bubble diameter for each gas flow condition was calculated and estimated for the individual bubble volume and total bubble number. The EDR by bubble wake was calculated as the product between the drag force (F_D) and terminal rise velocity (U_T) of an individual bubble as proposed by Chisti (2000) as follows:

$$\varepsilon_{wake|avg} = 6F_D U_T/0.8\pi d_B^3 \tag{10}$$

The drag force was calculated with Eq. (11), and the terminal rise velocity was calculated with Mandelson's equation (Eq. 12) (Chisti, 2000) as follows:

$$F_D = 2.6 U_T^2 \rho L A_b/2 \tag{11}$$

$$U_T = \sqrt{\frac{2\sigma}{d_B \rho_L} + 0.5 d_B g} \tag{12}$$

The projected area of an individual bubble was calculated with Eq. (13) using the previously measured diameters as follows:

$$A_b = \pi d_B^2/4 \tag{13}$$

Finally, an analysis of energy dissipated by bubble bursting was performed based on the methodology proposed by Walls (2017). In the analysis, the previously calculated bubble diameter distributions were first used to estimate the maximum energy dissipation rate by bubble bursting based on calculations performed in extant studies (Boulton-Stone & Blake, 1993; Garcia-Briones *et al*., 1994; Walls *et al*., 2017). Second, an estimation of

the volume of liquid surrounding a bubble that experienced a level of EDR above cellular damage was performed (Chalmers, 2015). A dimensionless EDR threshold was calculated (Eq. 14) by dividing the EDR level into a characteristic value that depends only on liquid properties such as viscosity, density, and surface tension. The liquid's parameters were estimated as reported values for LB broth with *E. coli* (Newton *et al*., 2016; Rühs *et al*., 2013). In the analysis proposed by Walls, the volume experiencing a determinate level of EDR can be calculated by relating the EDR threshold with a dimensionless parameter known as Lagrange (*La*). Specifically, *La* relates the bubble size with viscosity, inertia and capillarity (Eq. 15). Thus, *La* numbers were calculated with the bubble size distribution of each control system and were used to read the relative volume of liquid (V/V_b) experiencing an EDR of 1×10^6 W m^{-3} based on Walls' (2017) calculations.

$$\varepsilon_{burst|threshold} = \varepsilon_{burst}/\sigma^4\rho^2\mu^5 \quad (14)$$

$$La = \rho\sigma d_B/2\mu^2 \quad (15)$$

2.4 Statistical analysis

All the experiments were performed at least twice, and each sample was analyzed thrice (n = 6). Mean values ± standard errors were reported in the results. Statistically significant differences between groups were evaluated with one-way analysis of variance and Fisher's least significant difference (LSD) procedure at a confidence level of 95%.

3 Results and discussion

3.1 Development of the alternative system

The control system was developed based on the dynamics of DOT on a cell culture using *E. coli*. Thus, an open loop for the DOT dynamics was obtained to develop an algorithm that allows control of DOT with no variations on agitation speed or gas flow. The open loop for the alternative system and the respective biomass growth are shown in Fig. 1. Agitation and aeration were maintained constant during the runs, and thus there were no changes in k_La other than viscosification of the broth by increases in the biomass. When the culture grew and no control actions were performed, a total drop on

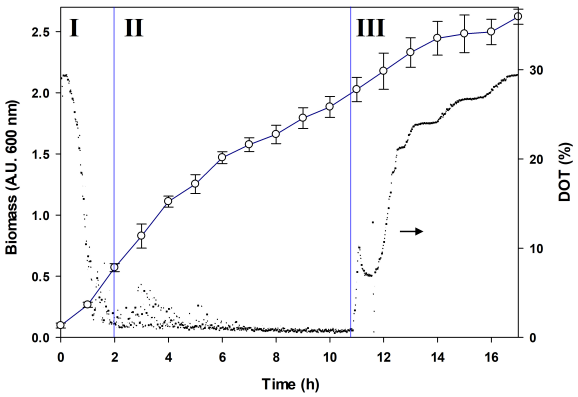

Figure 1. Biomass (*o*) and DOT (•) for an open-loop of *E. coli* in bioreactor. Agitation (600 rpm) and total gas flow (1.0 vvm) were maintained constant during the run and no DOT control system was used. Three oxygen consumption zones (I, II and III) are defined in the figure.

DOT was observed in the middle of the exponential phase, as it is expected for an oxygen-limited batch cultivation (Reynoso-Cereceda *et al*., 2016). Hence, it is evident the necessity of a control algorithm to maintain DOT levels when agitation speed and gas flow are maintained constant during a cell culture.

Oxygen dynamics during the open-loop were used to define three zones with similar behavior in terms of OUR (Fig. 1). Zone I was defined as the low uptake (OURI) zone and lasted for almost two hours in this experiment. The zone was characterized to exhibit the lowest OUR of the run due to low initial biomass concentration and low initial biomass growth rate. Following this, zone II corresponded to the highest OUR zone (OUR_{II}) and matched with the exponential increase in the biomass concentration at the maximum growth rate. A supply of oxygen is necessary because metabolism is significantly accelerated, and thus most control systems exhibit control problems in this zone (Diaz *et al*., 1995). Finally, at the end of the culture, the metabolism decreases and consumption of oxygen declines. Subsequently, the final oxygen consumption zone was determined to exhibit a lower oxygen uptake rate (OUR_{III}).

Hence, the three zones defined in the open-loop were used to develop the novel DOT control algorithm. Aerobic biological populations, such as bacteria, yeast, animal, and plant cells, exhibit similar behavior that can be fitted on OUR I, II, and III. For example, a similar kinetic of oxygen consumption has been reported for sensitive systems such as *Azadirachta*

indica and *Berveris vulgaris* cultures in STB (Orozco-Sánchez *et al*., 2011).

Although precise DOT control can be reached with commercial equipment, generally they manipulate variables that significantly perturbate k_La, such as agitation or aeration (Alford, 2006). Therefore, other control strategies must be performed to obtain an adequate DOT at constant gas flow, as it has been reported in extant studies (De León-Rodríguez *et al*., 2010; Trujillo Roldán *et al*., 2001). In the alternative control system, MFC for oxygen, nitrogen, and air were used in cascade as manipulated variables, responding to DOT changes, and maintaining a constant flow rate. Pairs of the gases were programmed into feedback control loops, and each *OUR* zone was matched with a specific loop. Table 1 shows the different PID loops that were programmed in the system, their variable pairing, and their control equations. First, a standard control loop (PID_{ref}) manipulating the opening time of a solenoid valve was used as a reference system. On the other hand, for the alternative system three control loops ($PID_{air/N2}$, $PID_{O2/N2}$, and $PID_{O2/air}$) were programed to manipulate the partial pressure of oxygen on the inlet gas albeit maintaining a constant total inlet gas flow. This was performed by allowing the PIDs to manipulate the flow of a MFC rich in oxygen and to complete the desired total gas flow (F_T) with other MFC on each sample time. A similar strategy was previously used for one MFC ($PID_{O2/N2}$) to control oscillating DOT on an *Azotobacter vinelandii* culture, and thereby obtaining an effective control (Trujillo Roldán *et al*., 2001). Subsequently, the same strategy was used for a one-compartment scale-down system and was proved in an *E. coli* culture by simulating DOT gradients at conditions with few hydrodynamic variations (De León-Rodríguez *et al*., 2010). However, these studies involved a reduced zone of k_La and DOT that is not sufficient for future studies on oxygen and momentum transfer in STB. Additionally, characterization on the liquid environment was not performed, and oxygen controllability was not quantified.

Fig. 2 shows the developed control algorithm used to match each OUR zone with a specific PID closed loop (selected by the user) and to automatically change loops among zones. The algorithm was designed for the operator to previously pair a specific PID loop with each OUR zone, based on the expected OUR. Subsequently, the operator must select control parameters (K_c, t_i, t_d) for each PID. The step is significantly important in the operation of the system because DOT controller actions can easily consider the process to oscillate, and destabilization problems can appear. It was reported that the tuning of DOT control systems is difficult due to fast changes of OUR and OTR as a result of biological activity (De León *et al*., 2001). However, methodologies for tuning rules in terms of the system structure, closed-loop and characteristic times have been reported to improved performance of PID feedback controllers in bioreactors (Aguilar *et al*., 2004).

Table 1. Equations for feedback control in a standard and an alternative DOT control system. Each control loop is defined in terms of the controlled and manipulated variables. For the alternative system, a complementary variable to maintain a constant total gas flow (F_T) is defined.

DOT control system	Loop name	Controlled variable	Manipulated variable	Complementary variable	Equations
Standard	PID_{std}	DOT	Solenoid valve opening time (t_v)	None	$t_v = t_{v_{t-1}} + K_c e + \frac{1}{t_i}\int e dt + t_d \frac{de}{dt}$
Alternative	PID_{Air/N_2}		Air mass flow (F_{Air})	Nitrogen mass flow (F_{N_2})	$F_{Air}(t) = F_{Air_{t-1}} + K_c e + \frac{1}{t_i}\int e dt + t_d \frac{de}{dt}$
					$F_{N_2}(t) = F_T - F_{Air}(t)$
	PID_{O_2/N_2}		Oxygen mass flow (F_{O_2})	Nitrogen mass flow (F_{N_2})	$F_{O_2}(t) = F_{O_{2t-1}} + K_c e + \frac{1}{t_i}\int e dt + t_d \frac{de}{dt}$
					$F_{N_2}(t) = F_T - F_{O_2}(t)$
	$PID_{O_2/Air}$		Nitrogen mass flow (F_{O_2})	Air mass flow (F_{Air})	$F_{O_2}(t) = F_{O_{2t-1}} + K_c e + \frac{1}{t_i}\int e dt + t_d \frac{de}{dt}$
					$F_{Air}(t) = F_T - F_{O_2}(t)$

*K_c, t_i and t_d correspond to the controller parameters constant gain, integral time and derivative time.

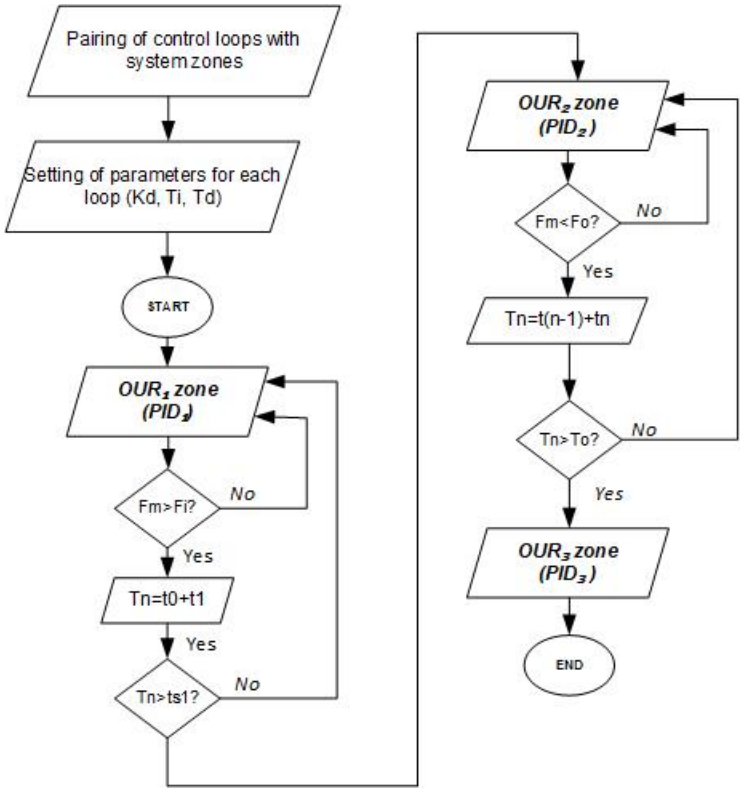

Figure 2. Algorithm for an alternative DOT control system that combines three PID loops by mixing air, oxygen, and nitrogen at a total constant gas flow during a cell cultivation in stirred tank bioreactor.

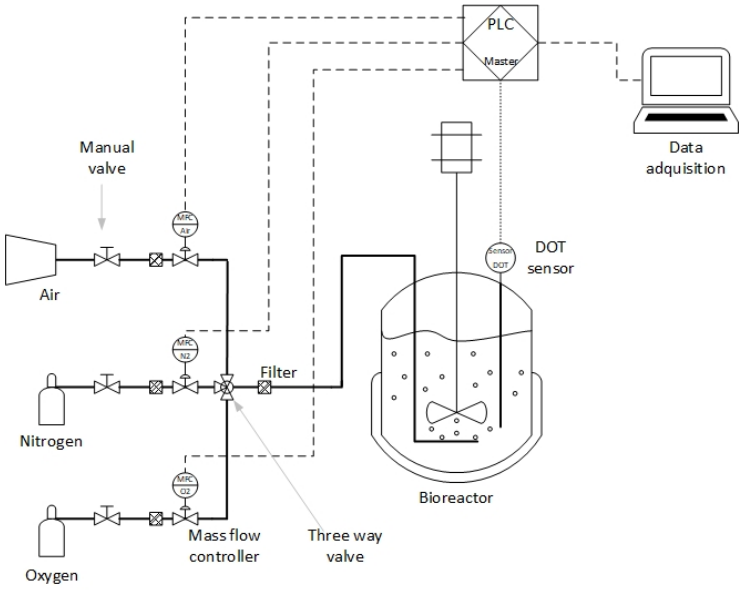

Figure 3. Configuration and instrumentation diagram of an alternative DOT control system for bioreactors that manipulates three mass flow controllers for oxygen, nitrogen, and air under a cascade control strategy.

After the operator selected the PID pairing and set control parameters, the control program was commenced by activating the first PID that will control DOT during the OURI zone. For the first change of zone, a flow limit (F_m) was established by the operator based on limitations on the use of the specific MFC. When the system reached the limit flow on the manipulated variable, a timer (T_n) commenced and OUR_I zone was changed to OUR_{II} after the determined time (t_{s1}) was realized. The same condition was necessary for the second change from OUR_{II} to OUR_{III}. Finally, Fig. 3 shows the instrumentation diagram of the alternative system for the control of DOT in STB using the developed algorithm. To the best of the authors' knowledge, current systems do not allow for the control of oxygen by using an algorithm like the proposed one, and the instrumentation diagram.

3.2 Evaluation of oxygen controllability

Results are provided for the cultivation of *E. coli* in bioreactor at 30% DOT by using a standard (Fig. 4-A, B) and the alternative (Fig. 4-C, D) control systems. Table 2 resumes operation and biological parameters for both cultures. Each system was syntonized to perform an adequate control of DOT at 30% by considering their own response time, control algorithm, and operation parameters. As shown in the table, relation aeration/agitation was different for each system, and thus the related parameters vary alongside (superficial gas velocity - SGV and P/V). With respect to the alternative system, it was possible to maintain constant agitation (500 rpm) and aeration (2 slpm) during the run. However, for the standard system, variation on the agitation/aeration was performed to allow modifications on OTR that diminished control error as much as possible.

It must be noted that the comparison made in the study is intended to be performed in terms of the control strategies as opposed to absolute values of the evaluated parameters. Indeed, both systems exhibited an effective performance because their maximum absolute error on DOT control was lower than 5.0%, and maximum biomass concentration and specific growth velocity were similar (Table 2). Furthermore, with the alternative system, a more precise control of DOT was reached during the entire cultivation ($e_{max} \approx$ 2%). Tight control of DOT have been reported in many extant studies by using other control systems (Arteaga Miñano & Vásquez Villalobos, 2012; Burke *et al*., 1998; Diaz *et al*., 1995; Gomes & Menawat, 2000; Mete *et al*., 2012; Trujillo Roldán *et al*., 2001).

The pairing of PID loops with OUR zones for the cultivation referenced in Fig. 4-D was performed as follows: $PID_{air/N2}$ for OUR_I, $PID_{O2/N2}$ for OUR_{II}, and $PID_{air/N2}$ for OUR_{III}. By using the previously described control algorithm (Fig. 2), the system changed each zone automatically as shown in Fig. 4-D. At the end of the OUR_I, the change of zone was performed by setting a limit F_i of 1.80 slpm on the air MFC during 1 min (t_{s1}). At this point, pure air was unable to maintain oxygen concentration because the biomass concentration of the culture increased. The culture then grew at the maximum rate, and thus oxygen was significantly consumed for 3 h. The consumption then diminished due to substrate depletion leading to preparation of the stationary phase. Maximum oxygen consumption was reached at 3 h. For a biological system with a higher OUR at the maximum stage, a control loop with $PID_{O2/air}$ can supply necessary oxygen for growth. After the maximum consumption of oxygen is reached, feeding of oxygen MFC decreases to low levels. Therefore, the second change in the zone is performed at 6.5 h (Fig. 4-D). The change is supported by oxygen saving when air is used as opposed to pure oxygen. Specifically, the alternative system can be potentially programmed to reach the control objective by using the minimum quantities of oxygen and nitrogen that are more expensive gases. Therefore, the system can be used for industrial applications.

As shown in Fig. 4-C, the change between PID loops (2 and 6 h) can induce peaks on DOT due to the algorithm conception itself. However, the peaks were rapidly softened by the control system, thereby implying a rapid response of the controller. It is reported that abrupt oscillations on DOT can be induced (for e.g., activation of regulons such as SoxRS on *E. coli* cultures that can decrease recombinant protein production rates or produce oxidative stress) (Akisue *et al*., 2018). Hence, it is necessary to develop systems that avoid DOT overshoots or control them at minimum time. The smooth control responses were reported by using fuzzy controllers (Akisue *et al*., 2018) or model adaptive control schemes (Chitra *et al*., 2018) that are complicated to develop and set up. An advantage of the alternative control system is that by using an automatic control algorithm with regular PID loops, it is not necessary to use model-based control systems to smooth controller responses.

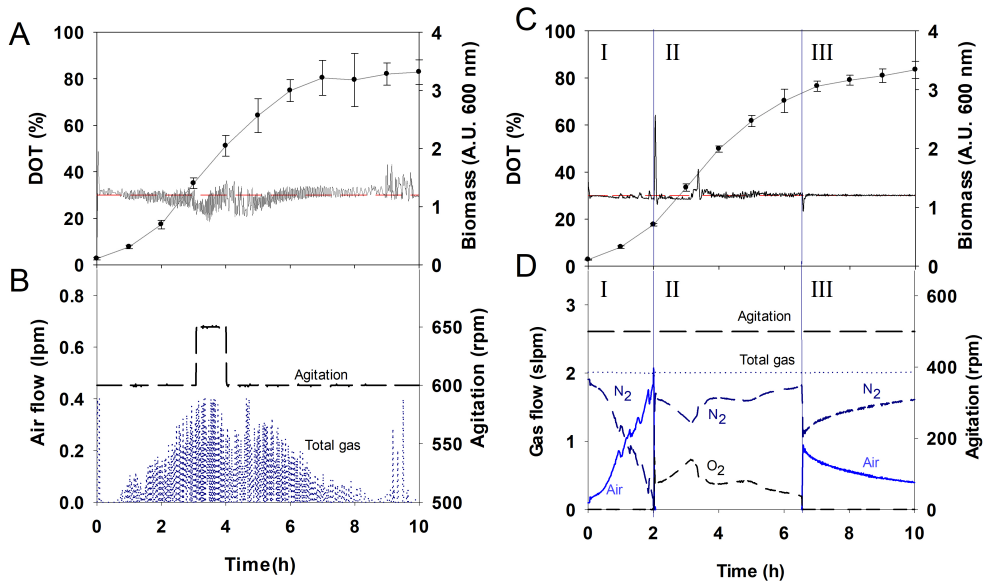

Figure 4. DOT (A, C-continuous dark line), *E. coli* biomass (A, C-line with marker), agitation speed (B, D), and gas flows (B, D) using a standard (A-B) and an alternative (C-D) system to control DOT at 30% in a stirred tank bioreactor.

Table 2. Operation parameters on the control of DOT at 30% using a standard and alternative systems for a 2-L stirred tank bioreactor with *E. coli* culture.

Parameter	Value for the culture	
	Standard system	Alternative system
N (rpm)	600 to 650	500
F_{gas} (slpm)	0.0 to 0.4	2
Maximum SGV (cm s^{-1})	0.5	2.7
P/V (W m^{-3})	148.1 to 465.6	57.9
X_{max} (OD_{600})	3.3 ± 0.2	3.4 ± 0.2
μ_{max} (h^{-1})	0.64 ± 0.02	0.62± 0.01
e_{max} (%)	4.3 ± 1.7	2.1 ± 0.3

Fig. 5 shows the characterization of the standard and alternative systems regarding DOT control error. The accumulated error is a variable that considers all individual errors for each sample time during the cultivation. As shown in Fig. 5-A, the alternative control system was able to control DOT with a lowest accumulated error starting from the middle of the exponential phase (4^{th} hour). This implies that the system developed in the study exhibited a 42% less accumulated error than a standard control strategy.

The increase in OUR during the exponential phase demands control systems to respond fast to small changes of k_La. At this phase, rapid changes in biomass concentration trigger destabilization of DOT (Fig. 4-A, C). The alternative system can stabilize the DOT faster (less than 1 h) in contrast to the standard strategy (almost 3 h). Additionally, at the stationary phase, the standard strategy increased its inefficiencies on control (Fig. 5-A) while the alternative system could stabilize the error after the middle of the exponential phase. To the best of the authors' knowledge, characterizations of DOT control systems are not usually reported in terms of accumulated or absolute control error. The errors are useful in analyzing the performance of any control system in terms of controllability (Ogata, 2010). Also, error quantification could be used to understand biological responses from cells. For example, control strategies have been found to highly influence the production of metabolites and recombinant proteins in *E. coli* when

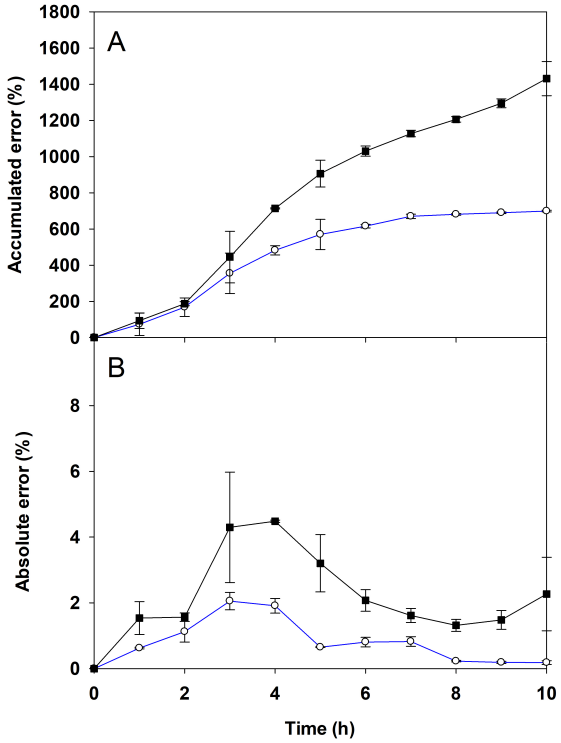

Figure 5. Accumulated (A) and absolute (B) errors on the DOT offset for a standard (■) and an alternative (o) DOT control systems operating on an *E. coli* cultivation in bioreactor at 30% DOT. Plotted points correspond to the mean of errors during each hour of the run.

evaluated at variations of 10% on DOT (Cheng *et al.*, 2021).

Conversely, Fig. 5-B shows the absolute errors at the different culture stages. Although both systems performed acceptable during the experiment (e_{max} < 5%), the alternative system performed below 2% of error as opposed to the standard during the exponential phase (3-6 h). Utsonomiya *et al.* (2003) studied the production of coproporphyrin by *Rhodobacter sphaeroides* under oxygen-controlled conditions in stirred bioreactors defining strict control of DOT within an error of 2.5%. However, low variations on DOT such as 1% have shown to generate changes on gene expression on the production of alginate by *Azotobacter vinelandii* (Díaz-Barrera *et al.*, 2017). To perform tight DOT control, Butkus *et al.* (2021) proposed an adaptative control system using a gain-scheduled approach. They simulated the controller performance and found a 0.063% absolute error for the adaptative system in opposition to 0.166% by

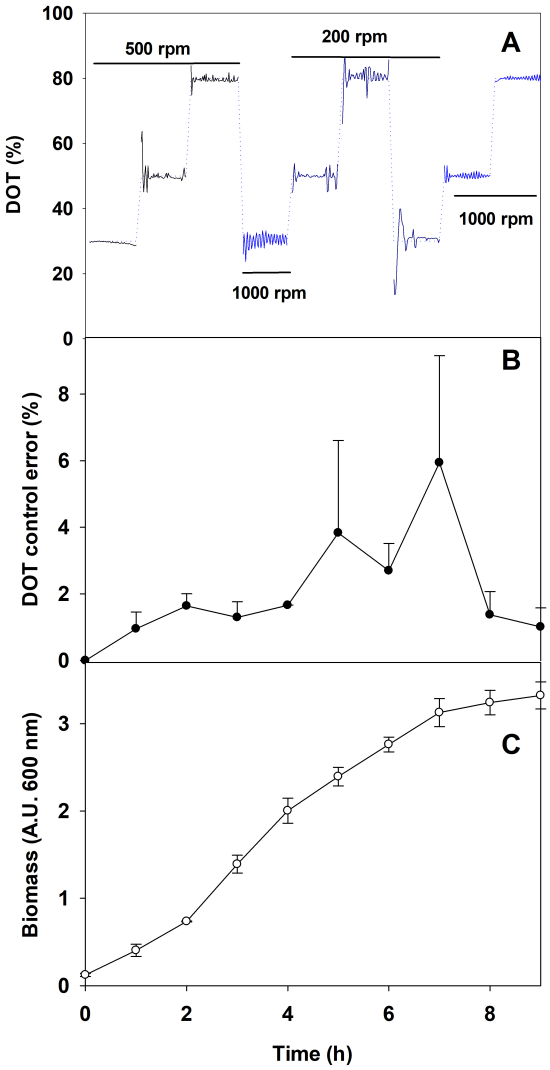

Figure 6. DOT (A), absolute error (B), and biomass (C) on an *E. coli* culture in bioreactor with perturbations on the set point (30, 50 and 80%) and agitation speed (200, 500, 1000 rpm) during the run. The DOT was controlled using an alternative control system at a constant total inlet gas flow.

a standard fixed PI controller. Nevertheless, gain-scheduling approaches are sensible to oxygen transfer conditions and models and may variate at high DOT conditions (Arevalo *et al.*, 2018).

The alternative system was also observed to effectively respond against perturbations other than biomass growth, such as changes on agitation and oxygen level. Fig. 6 shows the DOT on an *E. coli* culture when the system is perturbed on SP (30,

50, and 80%) and agitation speed (200, 500 and 1000 rpm), which correspond to initial k_La of 25, 75, and 178 h^{-1}, respectively (evaluated with 1 vvm of gas mixture). As shown in the Fig. 6-A, the system stabilized the oxygen response in a short period of time after each perturbation was applied, and total error was in average lower than 5% (Fig. 6-B). Indeed, the system was able to control DOT below 2% error, except during the middle of the exponential phase (from 5 to 7 h). This is opposed to the control performance on the previous experiment (Fig. 5) where control precision decreased between 3-5 h for both the standard and alternative system due to increasing in oxygen demand by the culture. Therefore, the behavior indicates possible control instabilities when operating the control system at a low k_La, in contrast with operating conditions where oxygen transfer is not limited (Fig. 6-A).

On the other hand, absolute error increased above 2% at the three evaluated setpoints during the stage at 200 rpm. This suggests that the agitation speed is a major challenge for the alternative system controllability, probably because its direct relationship with k_La.

Similar DOT control strategies using changes on set point during the cultivation have been found to enhance fumaric acid production by *Rhizopus orizae* (Fu *et al*., 2010), and increase recombinant protein expression in *E. coli* (Cheng *et al*., 2021). However, changes in kinetic growth of *E. coli* were not found in the experiment (Fig. 6-C).

3.3 Energy dissipation rates

To examine how the alternative control strategy affects the EDR in comparison with the standard strategy, both systems were characterized in terms of EDR related to agitation (Fig. 7-A, C), aeration (Fig. 7-D), and bubble explosion (Fig. 7-B). The EDR by agitation was practically constant when DOT was controlled with the alternative system (Fig. 7-C). The manipulated variable of the system corresponded to the partial pressure of oxygen in the inlet gas instead of agitation speed or gas flow, and thus the power input to the broth was unperturbed by effect of the controller (Serrano-Carreón *et al*., 2015). Conversely, the standard control system produced a wide range of noise in terms of EDR. The standard system modifies the total gas flow (using a solenoid valve as final control element) to reach a k_La that allows equilibrating the OTR with OUR at a certain DOT requirement, and thus dissipation energies varied nonuniformly with respect to the cultures. The knowledge on valve pulse effects on cells is not sufficient. However, bubble explosion is reported to exhibit negative consequences on plant and animal cell cultures (Chisti, 2000; Kieran *et al*., 2000). Effects are not reported on *E. coli* cultures because bacteria are not significantly sensitive to hydrodynamic stress due to their size (Trujillo-Roldán & Valdez-Cruz, 2006).

The accumulated EDR by agitation reached a maximum of 2 kJ/kg after 10 h of cultivation when DOT was controlled with the alternative system while the standard system delivered more than five times (10 kJ/kg) the quantity of energy to the broth. The energy must not cause growth problems with *E. coli* (Table 2 and Fig. 4-B) because hydrodynamic damage on bacteria is not reported at those values (Chamsartra *et al*., 2005; Hewitt *et al*., 1998). However, for plant and animal cell culture, affectations on cellular and metabolic processes were reported at the EDR values (Namdev & Dunlop, 1995). A study by Namdev & Dunlop (1995) indicated that for plant cell culture, different sublytic effects such as reduction of mitochondrial activity, regrowth capacity, and membrane activity can occur between 0.01 and 100 kJ/kg and that lytic effects are observed above the range. Conversely, Sowana *et al*. (2001) reported significant cell damage in cultures of carrot cells at a total energy dissipation corresponding to 10 kJ/kg.

The control system developed in the study can be used to culture different biological systems that are damaged from some EDR values. For example, insect cells at 0.01 kJ/kg, hybridoma at 0.1 kJ/kg, protozoa at 100 kJ/kg, and plant cells at 10000 kJ/kg on a STB suffer cell damage (Namdev & Dunlop, 1995). Furthermore, the system can be used to manipulate operation variables such that the production of secondary metabolites can be boosted. For example, cells of *Azadirachta indica* were reported to exhibit a higher metabolite production rate with certain mechanical stimulation when EDR increased from 0.49 to 1.51 W/kg (Villegas-Velásquez *et al*., 2017), and cells of *Rubia tinctorum* were observed to increase the production of anthraquinones when hydrodynamic stress was applied in a STB (Busto *et al*., 2008).

Therefore, although the alternative system can control DOT with only an EDR of 0.06 W/kg (Fig. 6-B), agitation speed, gas flow, or inlet oxygen concentration can be modified in the control set up and reach a desirable value of energy dissipation, thereby allowing biomass growth or metabolite production. Values obtained in Fig. 7 result from the configuration of the relation agitation/aeration for each system

(Table 2). However, as previously mentioned, the analysis in the study is related to the way the energy is delivered to media and on the dispersion of the energy as opposed to the absolute values obtained for each system. It must be noted that the developed system can be set to diminish the dispersion of energy for agitation to the broth.

Furthermore, it was even possible to manipulate the EDR via establishing adequate levels of agitation or gassing. Energy input would decrease from 0.10 to 0.05 W/kg if gas flow changed from 2 to 0.2 vvm. Conversely, EDR would increase from 0.001 to 0.418 W/kg if agitation changed from 100 to 1000 rpm. Thus, the alternative control system can be set with a specific relation aeration/agitation such that P/V or EDR can be manipulated without the expense of DOT control, and vice versa.

To compare the bubble diameter distributions, Fig. 7-B shows measurements at the operating conditions that were used for the alternative and the standard control strategies. Although both systems were set to work with the same sparger, geometry and media, bubble diameters for the standard control system were generally lower (0.06-0.18 cm) than for the alternative (0.09-0.35 cm). This difference is explained by the operative conditions that allowed effective control with each system. For example, the alternative controller operated at a high SGV since the gas flow was maintained at 2 slpm in comparison with the standard at 0-0.4 slpm (Table 2). Increasing gas flow rate implies a broaden bubble diameter distribution, as it was obtained in the experiment (Fig. 7-B). Simulations and validations of bubble formation under constant flow have been reported and would explain these results. Gerlach *et al*. (2007) found that bubble formation at constant volume occur until a certain flow rate value. On the contrary, at higher values, bubbles volume increases with gas flow rate.

Distribution of bubble diameters is an important operation condition that may generate physiological responses on cells because bubbles input energy to the broth when rising and bursting. In particular, mammalian and insect cell cultures have been reported for their susceptibility to damage via events derived from bubble hydrodynamics (Koynov *et al*., 2007). For example, Chisti (2000) reported a significant increase in the cellular death of *Spodoptera frugiperda* cell culture (insect cells) for average bubble diameters below 0.13 cm. On the other hand, Tran *et al*. (2016) studied the hydrodynamic extensional stress occurring for bubble diameters between 0.05-0.6 cm which is within the range of diameters used in this experiment. They found EDR values around the critical ones (104-105 W kg^{-1}) for suspended CHO cells at the higher value of the distribution interval.

Fig. 7-D shows the EDR that resulted when bubbles rose to the surface. The alternative control system operated at an average EDR of 40 kW/m^3_{wake}, in contrast with the standard system that operated at 176 kW m^{-3}_{wake}. The figure considers the effects of the distribution of bubble diameters and temporal effects due to pulses on gas flow. As shown in the figure, the standard system exhibits a broad interval on the energy via bubble wake, which can be shortened with the alternative system. Based on the analysis, in terms of EDR due to bubble wake, growth of *Spodoptera frugiperda* cell culture could be evaluated using the alternative control system on STB. Studies focused on operational maps that allow determination of operational conditions minimizing power consumption during an STB run have been done (Zheng *et al*., 2019). Also, control of aeration in an aerobic cultivations of *Saccharomyces cerevisiae* is reported to control the synthesis of chemical compounds of sensory importance in bioreactor (Estela-Escalante *et al*., 2012). Thus, the system developed in the study constitutes a useful approach to establish optimum operation variables to obtain minimum power consumption and maximize biomass growth or product production in a specific biological system.

Bubble diameters can be easily set on a control run independent of the type of controller since they are more influenced by the sparger. Nevertheless, the use of solenoid valves in control systems produces a perturbation due to the opening of the valve during each working time. This type of gas sparging perturbation is reported to produce lethal effects on hydrodynamic sensitive cell systems (Jöbses *et al*., 1991). Although the effects of solenoid valves on sensitive cells is not full characterized, it is known that an important cell damage can occur at the gas inlet region near the sparger (Liu *et al*., 2014). Smith & Davison (1990) reported a strategy to control DOT at constant shear in a plant cell bioreactor by using a set of solenoid valves that control the gas flow with rotameters on a fixed cycle time. Nevertheless, the study did not consider the possible effects of gas pulses near the impeller and among the liquid due to valve duty cycle. The pulse overflows produce peaks of energy that appear each time when a valve cycle is completed. Metabolic effects derived from gas flow perturbations and flow noise can be reduced by using MFCs as opposed to solenoid valves,

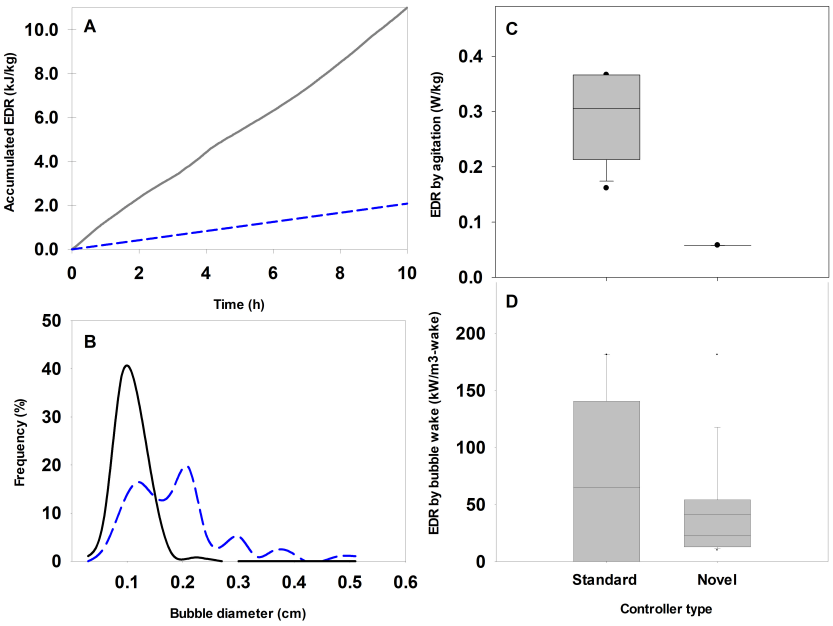

Figure 7. Accumulated energy dissipation by agitation (A), bubble diameter distribution (B), and average energy dissipation rates by agitation (C) and wake resulting from rising bubbles (D) on an *E. coli* culture in a bioreactor where the DOT is controlled by standard (straight line on figures A and B) and an alternative (dashed line on figure A and B) DOT control systems. Bar errors on C and D consider the variation due to aeration cycling and bubble diameter distribution on the run time, respectively.

Table 3. Estimated values of parameters that characterize an alternative and a standard DOT control systems in terms of energy effects via bubble bursting on an *E. coli* culture in bioreactor. Estimation is performed based on calculations made by Walls *et al*. (2017). Relative volume refers to volume of liquid surrounding a bubble experiencing an EDR corresponding to 1×10^6 W/m^3.

Parameter	Standard system	Alternative system
Bubble diameter range (cm)	0.06 - 0.18	0.09 - 0.35
$\varepsilon_{\max}$ by bubble wake (W/m^3)	$1 \times 10^{12} - 1 \times 10^{15}$	$1 \times 10^{12} - 1 \times 10^{14}$
Lagrange number	$3.48 \times 10^3 - 1.04 \times 10^4$	$5.21 \times 10^3 - 2.03 \times 10^4$
Relative volume V/V_b	Above 0.8	Above 0.2

used as manipulating devices. Thus, the effects of solenoid valves and their respective gas overflows in hydrodynamics can be examined by using the alternative control system developed in the study.

Table 3 shows the value of parameters estimated for the EDR via bubble bursting at the surface of the broth. There is an order or magnitude difference between the $\text{EDR}_{\max}$ as experienced by both cultures because it is determined that bubbles with lower diameters produce a higher EDR when they burst (Wu, 1995). However, Walls *et al*. (2017) estimated a solution for the $\text{EDR}_{\max}$ equations and indicated that the numerical solution extensively increased whenever the method was refined. Thus, they concluded that analysis of bubble bursting should be made in terms of a dimensionless parameter that considers the volume relation between liquid experiencing a level of EDR and bubble volume. In this study, a value of 1×10^6 W/m^3 was used to determine whether the distribution of bubble diameter that each system was observed to use in the control dynamics varied the levels of EDR experienced by cells. Thus, the alternative controller exhibited a lesser volumetric region of the broth fraction $V/V_b > 0.2$ that experienced an EDR_{burst} (1×10^6 W/kg) while the factor of the standard controller was higher, $V/V_b > 0.8$. Nevertheless, alternatives to improve mass transfer without increasing damage by bubble wake and bursting have been tested. For

example, in bubble columns, solid vector particles like Kraton have shown to improve oxygen transfer at different aeration rates, resulting in lower bubble rising velocities and higher gas holdup (Quijano *et al*., 2020).

Conclusions

In this work, an alternative DOT control system using a novel algorithm was developed and characterized for further study of oxygen and momentum transfer separately in stirred tank bioreactors. The system was found to precisely control DOT by changing the composition of the inlet gas. When compared to a standard commercial system, the results in the study indicated 41% less accumulated error on the *E. coli* culture at constant energy dissipation rate with respect to agitation (0.06 W kg^{-1}), and diminished variation of energy dissipated by bubble wake (49 kW/m^3_{wake}). Therefore, the alternative system can manipulate the aeration/agitation relationship such that specific EDR values are obtained without the expense of DOT control, and vice versa. Additionally, control was effectively performed at different agitation speeds (200, 500, and 1000 rpm), set points (30, 50 and 80% DOT), and culture phases. By using the alternative control system, sensitive cells (e.g., some plant or animal cells) could be cultivated in a stirred tank bioreactor under controlled momentum and oxygen transfer conditions. To the best of the authors' knowledge, this is the first characterization of a DOT control system at constant gas flow and agitation speed in terms of energy dissipation and control error.

Acknowledgments

The authors are grateful to Laboratorio de Bioconversiones (Grupo de Investigación Biotecnología Industrial) and to professor Hernán Darío Álvarez Zapata (Grupo de Investigación Kalman). Additionally, the authors acknowledge Dirección de Investigación of Universidad Nacional de Colombia for financial support for the project (Hermes 39417). Finally, the study was partially funded by "Programa de Apoyo a Proyectos de Investigación e Innovación Tecnológica, Universidad Nacional Autónoma de México" (PAPIIT-UNAM IT-200719, IN-208415).

Nomenclature

A_b	bubble projected area (m^2)
B	impeller clearance off the base (m)
C_{O2}	oxygen concentration (mg O_2 L^{-1})
C^*_{O2}	oxygen concentration in the gas-liquid interphase (mg O_2 L^{-1})
D	impeller diameter (m)
d_B	bubble diameter (m)
e	control error on the control system (%DOT)
F_x	mass flow for the gas "x" (slpm)
F_m	maximum gas flow set on a control algorithm (slpm)
F_i	gas flow on a control algorithm at the time i (slpm)
F_r	Froude number
F_{lg}	flow number
F_g	gas flow rate (mL min^{-1})
F_D	drag force (N)
g	gravitational acceleration (ms^{-2})
i	time of sample of the control system (min)
K_c	proportional constant on a PID loop
k_La	volumetric mass transfer coefficient on the liquid (h^{-1})
MFC	mass flow controller
SGV	superficial gas velocity (cm s^{-1})
N	agitation speed (s^{-1}, rpm)
OTR	oxygen transfer rate (mgO_2 L^{-1} h^{-1})
OUR	oxygen uptake rate (mgO_2 L^{-1} h^{-1})
PID_{std}	standard DOT control loop
$PID_{Air/N2}$	DOT control loop that manipulates a MFC of air and complements total gas flow with a MFC of nitrogen
$PID_{O2/N2}$	DOT control loop that manipulates a MFC of oxygen and complements total gas flow with a MFC of nitrogen
$PID_{O2/Air}$	DOT control loop that manipulates a MFC of oxygen and complements total gas flow with a MFC of air
P_o	power number
P	ungassed power input (W)
P_g	gassed power input (W)
P_c	calculated power input (W)
q_o	oxygen consumption rate (mgO_2 $mg^{-1}_{biomass}$ h^{-1})
t_n	time of evaluation of a control algorithm
t_i	integral time on a PID loop (min)
t_d	derivative time on a PID loop (min)
T	bioreactor vessel diameter (m)
T_o	parameter used to make the power equation dimensionless (1 m)
U_T	terminal rise velocity of a bubble (m s^{-1})

V_c	controlled variable on a control loop
V_m	manipulated variable on a control loop
V_f	variable used to maintain constant flow on a DOT control loop
V_L	working volume (m^3)
X	biomass concentration (g L^{-1})
x	impeller disk thickness (m)
ε	energy dissipation rate (W kg^{-1})
ρ	broth density (kg m^{-3})
ρ_L	liquid density (kg m^{-3})
σ	gas-liquid interfacial tension (N m^{-1})
μ	liquid viscosity (Pa s)

References

Aguilar, R., Soto, G., Martínez, S., & Maya-Yescas, R. (2004). Substrate regulation in fixed bed bioreactors via feedback control. *Revista Mexicana de Ingeniería Química 3*, 1-11.

Akesson, M., & Hagander, P. (1998). *Control of Dissolved Oxygen in Stirred Bioreactors* (Technical Reports TFRT-7571). https://portal.research.lu.se/portal/files/4770852/8727192.pdf

Akisue, R. A., Horta, A. C. L., & de Sousa, R. J. (2018). Development of a fuzzy system for dissolved oxygen control in a recombinant *Escherichia coli* cultivation for heterologous protein expression. *Proceedings of the 28th European Symposium on Computer Aided Process Engineering*. June 10th to 13th, 2018, Graz, Austria., 43, 1129-1134. https://doi.org/10.1016/B978-0-444-64235-6.50197-2

Alford, J. S. (2006). Bioprocess control: Advances and challenges. *Computers and Chemical Engineering 30(10-12)*, 1464-1475. https://doi.org/10.1016/j.compchemeng.2006.05.039

Arevalo, H., Sanchez, F., Ruiz, F., Guerrero, D., Patino, D., Almeciga-Diaz, C. J., & Rodriguez-Lopez, A. (2018). Gain-scheduled oxygen concentration control system for a bioreactor. *IEEE Latin America Transactions 16(11)*, 2689-2697. https://doi.org/10.1109/TLA.2018.8795109

Arteaga Miñano, H., & Vásquez Villalobos, V. (2012). Control difuso del oxígeno disuelto, pH y temperatura de un biorreactor columna de burbujas en la producción de biomasa de *Candida utilis*. *Scientia Agropecuaria 2*, 139-148.

Boulton-Stone, J. M., & Blake, J. R. (1993). Gas bubbles bursting at a free surface. *Journal of Fluid Mechanics 254(I)*, 437-466. https://doi.org/10.1017/S0022112093002216

Bujalski, W. (1986). *Three phase mixing: studies of geometry, viscosity and scale*. Doctoral Dissertation. ISNI: 0000 0001 2442 4498. [University of Birmingham]. https://ethos.bl.uk/OrderDetails.do?uin=uk.bl.ethos.323109

Burke, P. V., Kwast, K. E., Everts, F., & Poyton, R. O. (1998). A fermentor system for regulating oxygen at low concentrations in cultures of *Saccharomyces cerevisiae*. *Applied and Environmental Microbiology 64(3)*, 1040-1044.

Busto, V. D., Rodríguez-Talou, J., Giulietti, A. M., & Merchuk, J. C. (2008). Effect of shear stress on anthraquinones production by *Rubia tinctorum* suspension cultures. *Biotechnology Progress 24(1)*, 175-181. https://doi.org/10.1021/bp0702370

Butkus, M., Levišauskas, D., & Galvanauskas, V. (2021). Simple gain-scheduled control system for dissolved oxygen control in bioreactors. *Processes 9(9)*. https://doi.org/10.3390/pr9091493

Chalmers, J. J. (2015). Mixing, aeration and cell damage, 30+ years later: What we learned, how it affected the cell culture industry and what we would like to know more about. *Current Opinion in Chemical Engineering 10*, 94-102. https://doi.org/10.1016/j.coche.2015.09.005

Chamsartra, S., Hewitt, C. J., & Nienow, A. W. (2005). The impact of fluid mechanical stress on Corynebacterium glutamicum during continuous cultivation in an agitated bioreactor. *Biotechnology Letters 27(10)*, 693-700. https://doi.org/10.1007/S10529-005-4690-5

Cheng, L., Zhao, C., Yang, X., Song, Z., Lin, C., Zhao, X., Wang, J., Wang, J., Wang,

L., Xia, X., & Shen, Z. (2021). Application of a dissolved oxygen control strategy to increase the expression of *Streptococcus suis* glutamate dehydrogenase in *Escherichia coli*. *World Journal of Microbiology and Biotechnology 37(4)*, 1-9. https://doi.org/10.1007s11274-021-03025-2

Chisti, Y. (2000). Animal-cell damage in sparged bioreactors. *Trends in Biotechnology 18(10)*, 420-432. https://doi.org/10.1016/S0167-7799(00)01474-8

Chitra, M., Pappa, N., & Abraham, A. (2018). Dissolved oxygen control of batch bioreactor using model reference adaptive control scheme. *IFAC-PapersOnLine 51(4)*, 13-18. https://doi.org/10.1016/j.ifacol.2018.06.008

De León-Rodríguez, A., Galindo, E., & Ramírez, O. T. (2010). Design and characterization of a one-compartment scale-down system for simulating dissolved oxygen tension gradients. *Journal of Chemical Technology and Biotechnology 85(7)*, 950-956. https://doi.org/10.1002/jctb.2384

De León, A., Barba-De La Rosa, A. P., Mayani, H., Galindo, E., & Ramírez, O. T. (2001). Two useful dimensionless parameters that combine physiological, operational and bioreactor design parameters for improved control of dissolved oxygen. *Biotechnology Letters 23(13)*, 1051-1056. https://doi.org/10.1023/A:1010598121587

Devi, T. T., & Kumar, B. (2017). Mass transfer and power characteristics of stirred tank with Rushton and curved blade impeller. *Engineering Science and Technology, an International Journal 20(2)*, 730-737. https://doi.org/10.1016/J.JESTCH.2016.11.005

Díaz-Barrera, A., Maturana, N., Pacheco-Leyva, I., Martínez, I., & Altamirano, C. (2017). Different responses in the expression of alginases, alginate polymerase and acetylation genes during alginate production by *Azotobacter vinelandii* under oxygen-controlled conditions. *Journal of Industrial Microbiology and Biotechnology 44(7)*, 1041-1051. https://doi.org/10.1007/s10295-017-1929-9

Diaz, C., Dieu, P., Feuillerat, C., Lelong, P., & Salome, M. (1995). Adaptive predictive control of dissolved oxygen concentration in a laboratory-scale bioreactor. *Journal of Biotechnology 43(1)*, 21-32. https://doi.org/10.1016/0168-1656(95)00101-5

Doran, P. M. (1995). 7 - Fluid flow and mixing. In *Bioprocess Engineering Principles* (pp. 129-163). Elsevier. https://doi.org/10.1016/B978-012220855-3/50007-9

Dunlop, E. H., & Namdev, P. K. (1994). Effect of fluid shear forces on plant cell suspensions. *Chemical Engineering Science 49(14)*, 2263-2276. https://doi.org/10.1016/0009-2509(94)E0043-P

Estela-Escalante, W., Rychtera, M., Melzoch, K., & Hatta-Sakoda, B. (2012). Effect of aeration on the fermentative activity of *Saccharomyces cerevisiae* culture in apple juice. *Revista Mexicana de Ingeniería Química 11(2)*, 211-226.

Ferreira, A., Rocha, F., Mota, A., & Teixeira, J. A. (2017). 19- Characterization of Industrial Bioreactors (Mixing, Heat, and Mass Transfer). In *Current Developments in Biotechnology and Bioengineering: Bioprocesses, Bioreactors and Controls* (pp. 563-592). Elsevier. https://doi.org/10.1016/B978-0-444-63663-8.00019-7

Fu, Y. Q., Li, S., Chen, Y., Xu, Q., Huang, H., & Sheng, X. Y. (2010). Enhancement of fumaric acid production by Rhizopus oryzae using a two-stage dissolved oxygen control strategy. *Applied Biochemistry and Biotechnology 162(4)*, 1031-1038. https://doi.org/10.1007/s12010-009-8831-5

Garcia-Briones, M. A., Brodkey, R. S., & Chalmers, J. J. (1994). Computer simulations of the rupture of a gas bubble at a gas-liquid interface and its implications in animal cell damage. *Chemical Engineering Science 49(14)*, 2301-2320. https://doi.org/10.1016/0009-2509(94)E0038-R

García-Cabrera, R. I., Valdez-Cruz, N. A., Daniel-Vázquez, A., Blancas-Cabrera, A., & Trujillo-Roldán, M. A. (2021). Roles of culture media and oxygen transfer in the scale-up from shake flasks to pneumatic bioreactor of the plant growth-promoting bacterium *Rhizobium*

phaseoli. Revista Mexicana de Ingeniería Química 20(2), 1091-1109.

García-Ochoa, F., Escobar, S., & Gómez, E. (2015). Specific oxygen uptake rate as indicator of cell response of *Rhodococcus erythropolis* cultures to shear effects. *Chemical Engineering Science 122*, 491-499. https://doi.org/10.1016/j.ces.2014.10.016

Garcia-Ochoa, Félix, & Gomez, E. (2009). Bioreactor scale-up and oxygen transfer rate in microbial processes: An overview. *Biotechnology Advances 27(2)*, 153-176. https://doi.org/10.1016/j.biotechadv.2008.10.006

Garcia-Ochoa, Felix, Gomez, E., Santos, V. E., & Merchuk, J. C. (2010). Oxygen uptake rate in microbial processes: An overview. *Biochemical Engineering Journal 49(3)*, 289-307. https://doi.org/10.1016/j.bej.2010.01.011

Gerlach, D., Alleborn, N., Buwa, V., & Durst, F. (2007). Numerical simulation of periodic bubble formation at a submerged orifice with constant gas flow rate. *Chemical Engineering Science 62*, 2109-2125. https://doi.org/10.1016/j.ces.2006.12.061

Gezork, K. M., Bujalski, W., Cooke, M., & Nienow, A. W. (2000). The transition from homogeneous to heterogeneous flow in a gassed, stirred vessel. *Chemical Engineering Research and Design 78(3)*, 363-370. https://doi.org/10.1205/026387600527482

Gill, N. K., Appleton, M., Baganz, F., & Lye, G. J. (2008). Quantification of power consumption and oxygen transfer characteristics of a stirred miniature bioreactor for predictive fermentation scale-up. *Biotechnology and Bioengineering 100(6)*, 1144-1155. https://doi.org/10.1002/bit.21852

Gomes, J., & Menawat, A. S. (2000). Precise control of dissolved oxygen in bioreactors - a model-based geometric algorithm. *Chemical Engineering Science 55(1)*, 67-78. https://doi.org/10.1016/S0009-2509(99)00305-X

Hewitt, C. J., Boon, L. A., Mcfarlane, C. M., & Nienow, A. W. (1998). The use of flow cytometry to study the impact of fluid mechanical stress on *Escherichia coli* W3110 during continuous cultivation in an agitated bioreactor. *Biotechnology and Bioengineering 59(5)*, 612-620.

Hua, J., Erickson, L. E., Yiin, T. Y., & Glasgow, L. a. (1993). A review of the effects of shear and interfacial phenomena on cell viability. *Critical Reviews in Biotechnology 13(4)*, 305-328. https://doi.org/10.3109/07388559309075700 Jöbses, I., Martens, D., & Tramper, J. (1991). Lethal events during gas sparging in animal cell culture. *Biotechnology and Bioengineering 37(5)*, 484-490. https://doi.org/10.1002/bit.260370510

Kieran, P. M., Malone, D. M., & MacLoughlin, P. F. (2000). Effects of hydrodynamic and interfacial forces on plant cell suspension systems. *Advances in Bochemical Engineering/Biotechnology 67*, 139-177. https://doi.org/10.1007/3-540-47865-5_5

Koynov, A., Tryggvason, G., & Khinast, J. G. (2007). Characterization of the localized hydrodynamic shear forces and dissolved oxygen distribution in sparged bioreactors. *Biotechnology and Bioengineering 97(2)*, 317-331). https://doi.org/10.1002/bit.21281

Liu, Y., Li, F., Hu, W., Wiltberger, K., & Ryll, T. (2014). Effects of bubble-liquid two-phase turbulent hydrodynamics on cell damage in sparged bioreactor. *Biotechnology Progress 30(1)*, 48-58. https://doi.org/10.1002/btpr.1790

Maia, C. I., Fonseca, M. M. R., Vasconcelos, J. M. T., Alves, S. S., & Mora, A. (1999). Effect of antifoam addition on gas-liquid mass transfer in stirred fermenters. *Bioprocess Engineering 20*, 165-172.

Martínez-Hernández, S. L., Marín-Muñoz, M. A., Ventura-Juárez, J., & Jáuregui-Rincón, J. (2020). Fed-batch cultivation and operational conditions for the production of a recombinant anti-amoebic vaccine in *Pichia pastoris* system. *Revista Mexicana de Ingeniería Química 19(2)*, 691-705.

Martinov, M., Gancel, F., Jacques, P., Nikov, I., & Vlaev, S. (2008). Surfactant effects on aeration

performance of stirred tank reactors. *Chemical Engineering & Technology 31(10)*, 1494-1500. https://doi.org/10.1002/CEAT.200700401

Mete, T., Ozkan, G., Hapoglu, H., & Alpbaz, M. (2012). Control of dissolved oxygen concentration using neural network in a batch bioreactor. *Computer Applications in Engineering Education 20(4)*, 619-628. https://doi.org/10.1002/cae.20430

Namdev, P. K., & Dunlop, E. H. (1995). Shear sensitivity of plant cells in suspensions present and future. *Applied Biochemistry and Biotechnology 54(1-3)*, 109-131. https://doi.org/10.1007/BF02787914

Neunstoecklin, B., Villiger, T. K., Lucas, E., Stettler, M., Broly, H., Morbidelli, M., & Soos, M. (2015). Pilot-scale verification of maximum tolerable hydrodynamic stress for mammalian cell culture. *Applied Microbiology and Biotechnology 100(8)*, 3489-3498. https://doi.org/10.1007/s00253-015-7193-x

Newton, J. M., Schofield, D., Vlahopoulou, J., & Zhou, Y. (2016). Detecting cell lysis using viscosity monitoring in *E. coli* fermentation to prevent product loss. *Biotechnology Progress 32(4)*, 1069-1076. https://doi.org/10.1002/btpr.2292

Nienow, A. W. (1998). Hydrodynamics of stirred bioreactors. *Applied Mechanics Reviews 51(1)*, 3. https://doi.org/10.1115/1.3098990

Ogata, K. (2010). *Modern Control Engineering* (P. Hall (ed.); 5th ed.). Pearson.

Orozco-Sánchez, F., Sepúlveda-Jiménez, G., Trejo-Tapia, G., Zamilpa, A., & Rodríguez-Monroy, M. (2011). Oxygen limitations to grow *Azadirachta indica* cell culture in shake flasks. *Revista Mexicana de Ingeniera Qumica 10(3)*, 343-352.

Quijano, G., Franco-Morgado, M., Córdova-Aguilar, M. S., Galindo, E., & Thalasso, F. (2020). Oxygen transfer in a three-phase bubble column using solid polymers as mass transfer vectors. *Revista Mexicana de Ingeniería Quimica 19(3)*, 483-494. https://doi.org/10.24275/rmiq/Proc1486

Raffo-Durán, J., Figueredo-Cardero, A., & Dustet-Mendoza, J. C. (2014). Características de la hidrodinámica de un biorreactor industrial tipo tanque agitado. *Revista Mexicana de Ingeniería Química 13(3)*, 823-839.

Reynoso-Cereceda, G. I., Garcia-Cabrera, R. I., Valdez-Cruz, N. A., & Trujillo-Roldán, M. A. (2016). Shaken flasks by resonant acoustic mixing versus orbital mixing: Mass transfer coefficient k_La characterization and *Escherichia coli* cultures comparison. *Biochemical Engineering Journal 105*, 379-390.

Rühs, P. A., Böni, L., Fuller, G. G., Inglis, R. F., & Fischer, P. (2013). In-situ quantification of the interfacial rheological response of bacterial biofilms to environmental stimuli. *PLOS ONE 8(11)*. https://doi.org/10.1371/journal.pone.0078524

Schaepe, S., Kuprijanov, A., Sieblist, C., Jenzsch, M., Simutis, R., & Lübbert, A. (2013). k_La of stirred tank bioreactors revisited. *Journal of Biotechnology 168(4)*, 576-583. https://doi.org/10.1016/j.jbiotec.2013.08.032

Schlüter, V., & Deckwer, W. D. (1992). Gas/liquid mass transfer in stirred vessels. *Chemical Engineering Science 47(9-11)*, 2357-2362. https://doi.org/10.1002/aic.690361121

Serrano-Carreón, L., Galindo, E., Rocha-Valadéz, J. A., Holguín-Salas, A., & Corkidi, G. (2015). Hydrodynamics, Fungal Physiology, and Morphology. *Advances in Biochemical Engineering/Biotechnology 149*, 55-90. https://doi.org/10.1007/10_2015_304

Smith, J. M. (2006). Large multiphase reactors: Some open questions. *Chemical Engineering Research and Design 84(4 A)*, 265-271. https://doi.org/10.1205/cherd05055

Smith, J. M., Davison, S. W., & Payne, G. F. (1990). Development of a strategy to control the dissolved concentrations of oxygen and carbon dioxide at constant shear in a plant cell bioreactor. *Biotechnology and Bioengineering 35(11)*, 1088-1101. https://doi.org/10.1002/bit.260351104

Sowana, D. D., Williams, D. R. G., Dunlop, E. H., Dally, B. B., O'Neill, B. K., & Fletcher, D. F.

(2001). Turbulent shear stress effects on plant cell suspension cultures. *Chemical Engineering Research and Design 79(8)*, 867-875. https://doi.org/10.1205/02638760152721370

Tran, T. T., Lee, E. G., Lee, I. S., Woo, N. S., Han, S. M., Kim, Y. J., & Hwang, W. R. (2016). Hydrodynamic extensional stress during the bubble bursting process for bioreactor system design. *Korea-Australia Rheology Journal 28(4)*, 315-326. https://doi.org/10.1007/s13367-016-0032-5

Trujillo-Roldán, M. A., & Valdez-Cruz, N. A. (2006). El estrés hidrodinámico: Muerte y daño celular en cultivos agitados. *Revista Latinoamericana de Microbiología 48(3-4)*, 269-280.

Trujillo Roldán, M. A., Peña, C., Ramirez, O. T., & Galindo, E. (2001). Effect of oscillating dissolved oxygen tension on the production of alginate by *Azotobacter vinelandii*. *Biotechnology Progress 17(6)*, 1042-1048. https://doi.org/10.1021/bp010106d

Utsunomiya, T., Tanaka, T., Tanaka, T., Watanabe, M., & Sasaki, K. (2003). Coproporphyrin production by *Rhodobacter sphaeroides* under aerobic in the dark and dissolved-oxygen-controlled conditions. *World Journal of Microbiology and Biotechnology 19(2)*, 227-231. https://doi.org/10.1023/A:1023257228152

Villegas-Velásquez, S., Martínez-Mira, A. D., Hoyos, R., Rojano, B., & Orozco-Sánchez, F. (2017). Hydrodynamic stress and limonoid production in *Azadirachta indica* cell culture. *Biochemical Engineering Journal 122*, 75-84. https://doi.org/10.1016/j.bej.2017.03.004

Walls, P. L. L., McRae, O., Natarajan, V., Johnson, C., Antoniou, C., & Bird, J. C. (2017). Quantifying the potential for bursting bubbles to damage suspended cells. *Scientific Reports 7(1)*, 1-9. https://doi.org/10.1038/s41598-017-14531-5

Warmoeskerken, M. M. C. G., & Smith, J. M. (1982). Description of the power curves of turbine stirred gas dispersions. *Proceedings of the 4th European Conference of Mixing*, 237-246.

Wu, J. (1995). Mechanisms of animal cell damage associated with gas bubbles and cell protection by medium additives. *Journal of Biotechnology 43(2)*, 81-94. https://doi.org/10.1016/0168-1656(95)00133-7

Zheng, C., Guo, J., Wang, C., Chen, Y., Zheng, H., Yan, Z., & Chen, Q. (2019). Experimental study and simulation of a three-phase flow stirred bioreactor. *Chinese Journal of Chemical Engineering 27(3)*, 1-11. https://doi.org/10.1016/j.cjche.2018.06.010